Prediction of Vortex Flow Characteristics of Wings at Subsonic and Supersonic Speeds

John E. Lamar*
NASA Langley Research Center, Hampton, Va.

The leading-edge suction analogy of Polhamus, which has been successful in the prediction of vortex lift characteristics on wings with pointed tips at subsonic and supersonic speeds, has recently been extended to account for the vortex flow characteristics for wings with side edges. Comparisons of experimental data and other currently used methods with the extended method are made for wings having side edges at subsonic and supersonic speeds. Recent data obtained for a low-aspect-ratio cropped-delta wing with various amounts of asymmetrical tip rake, simulating a roll control device, are also presented.

Nomenclature

A = aspect ratio
B = $(M^2-1)^{1/2}$
b = wing span
C_D = drag coefficient, (drag/$q_\infty S_{ref}$)
$C_{D,o}$ = experimental value of drag coefficient at $C_L=0$
C_L = lift coefficient, (lift/$q_\infty S_{ref} b$)
C_l = rolling-moment coefficient; (rolling moment/$q_\infty S_{ref} b$)
C_m = pitching-moment coefficient about the reference point; and unless otherwise stated is located at ($c_{ref}/4$),(pitching moment/$q_\infty S_{ref} c_{ref}$)
C_N = normal-force coefficient, (normal force/$q_\infty S_{ref}$)
$\Delta C_{p,u}$ = change in upper surface pressure coefficient from $\alpha=0°$, (change in upper surface pressure/q_∞)
c = streamwise chord
c_n = section normal-force coefficient, (section normal force/$q_\infty c$)
c_t' = $\frac{c_t}{b/2}\cot\Lambda$
E = complete elliptic integral of the second kind with modulus $[1-(B\cot\Lambda)^2]^{1/2}$
f_M = leading-edge length correction factor due to subsonic Mach number, $\sec\Lambda/(B^2+\tan^2\Lambda)^{1/2}$
g = acceleration due to gravity
K_p = potential-lift factor, $\partial(C_{N,p})/\partial(\sin\alpha\cos\alpha)$
$K_{v,le}$ = leading-edge-vortex-lift factor,

$$\frac{\partial\left(\frac{2\text{ leading-edge suction force from one edge}}{q_\infty S_{ref}}\right)}{\partial\sin^2\alpha}$$

$K_{v,se}$ = side-edge-vortex-lift facor,

$$\frac{\partial\left(\frac{2\text{ side-edge suction force from one edge}}{q_\infty S_{ref}}\right)}{\partial\sin^2\alpha}$$

$K_{v,tot}$ = $(K_{v,le}/f_m)+K_{v,se}$
M = Mach number of the freestream
m = $B\cot\Lambda$
q_∞ = freestream dynamic pressure
S_{ref} = reference area
U = freestream velocity
u = induced velocity in the X-direction at a point (x,y)
v = induced velocity in the Y-direction at a point (x,y)
x,y = distances from a coordinate origin located at the leading-edge apex; x positive downstream and y positive toward the right wing tip
x/c = fractional distance along a streamwise chord
Δx = distance along the tip chord to the centroid of the side-edge-vortex lift
α = angle of attack, deg
β = $(1-M^2)^{1/2}$
γ = distributed bound vorticity at a point (x,y)
δ = distributed trailing vorticity at a point (x,y)
δ_t = tip rake angle, positive trailing-edge tip moves inboard
Λ = leading-edge sweep angle, positive for sweepback, degrees
λ = taper ratio, c_t/c_r
μ = $\sin^{-1}(1/M)$

Subscripts

c = centroid
i = particular item or location
le = leading edge
p = potential or attached flow
r = root
ref = reference
se = side edge
t = tip
tot = total
vle = vortex effect at the leading edge
vse = vortex effect at the side edge

Presented as Paper 75-249 at the AIAA 13th Aerospace Sciences Meeting, Pasadena, Calif., January 20-22, 1975; submitted March 4, 1975; revision received July 17, 1975.

Index categories: Aircraft Aerodynamics (including Component Aerodynamics); Aircraft Handling, Stability and Control; Subsonic and Transonic Flow.

*Aeronautical Research Scientist, Applied Aerodynamics Section, Fluid Dynamics Branch, Subsonic-Transonic Aerodynamics Division. Member AIAA.

Introduction

VORTEX flows, such as those associated with edge separation along with the accompanying flow reattachment, are encountered at many points within the flight and maneuver envelopes of high-speed aircraft. If analytical methods for the design and analysis of aircraft are to be completely reliable, it will be necessary to provide accurately for the effects of these separated flows.

The leading-edge-suction analogy of Polhamus,[1] though not theoretically proven, has provided good predictions of the overall forces and pitching moment for slender wings with pointed tips of interest for supersonic cruise vehicles. For the more general trapezoidal wings of interest for fighter type aircraft, however, it is necessary to take into account the separation along the side edges (finite tip chords).

Figure 1 presents the wing aerodynamic characteristics at $M=0.2$ of a representative fighter aircraft having a cropped arrow planform with sharp leading and side edges. At a C_L

corresponding to a 1-g cruise load factor, the combination of potential flow theory and leading-edge-vortex lift can be seen on both graphs to estimate reasonably well the experimental data of Ref. 2. However, at a C_L corresponding to the 7-g maneuvering load factor, it is clear that the theoretical combination underestimates the data. This paper takes the viewpoint that the unaccounted effect can be attributed to the vortex lift originating along the side edges, and that this effect can be estimated by employing a suction analogy similar to that used at the leading edge. It is the purpose of this paper to explore such an approach.

Concept of Side-Edge-Vortex Lift

The concept of generating vortex lift at the leading edges of wings is given by Polhamus[1] and is called the leading-edge-suction analogy. It is based on the singular nature of the induced-tangential velocity at the leading edge, producing a finite leading-edge-suction force in the chord plane for potential or attached flow. If the flow separates in going around the leading edge and forms into a shed vortex which causes the flow to reattach to the leeward surface, hereafter called vortex flow, then the potential-flow-suction force no longer acts in the chord plane but instead in the normal-force direction.

The suction analogy concept is not limited to vortex flows around the leading edge but can be applied wherever singularities in the potential-flow-induced velocities produce an edge force. Figure 2 shows that this can occur along the side edges due to the singularities in v; hence, with vortex flows around the side edges, the side forces will act in the normal-force direction, also.

A mathematical procedure for computing this side force has been developed, initially, for wings at subsonic speeds and is given in Ref. 2. The procedure employs the modified Multhopp method of Ref. 3 to provide the information needed to begin the side-force computation. The effect of the side-edge-vortex lift is combined with that from the leading edge and potential flow effect to yield estimates which will be denoted as being those of the present method.

Bradley[4] also uses the suction analogy to estimate the subsonic side-edge-vortex lift, but employs a vortex-lattice method to obtain the potential-flow-side forces. In general, the results obtained with the method of Ref. 4 and those of the present method are in very good agreement.

The following equations relate the potential- and vortex-lift factors to C_L, C_D, and C_m

$$C_L = \overbrace{K_p \sin\alpha \cos^2\alpha}^{C_{L,p}} + \overbrace{K_{v,le} \sin^2\alpha \cos\alpha}^{C_{L,vle}} + \overbrace{K_{v,se} \sin^2\alpha \cos\alpha}^{C_{L,vse}} \tag{1}$$

or

$$C_L = K_p \sin\alpha \cos^2\alpha + K_{v,tot} \sin^2\alpha \cos\alpha \tag{2}$$

$$C_D = C_{D,o} + C_L \tan\alpha = C_{d,o} + K_p \sin^2\alpha \cos\alpha + K_{v,tot} \sin^3\alpha \tag{3}$$

and

$$C_m = \overbrace{K_p \sin\alpha \cos\alpha (\bar{x}_p/c_{ref})}^{C_{m,p}} + \overbrace{K_{vle} \sin^2\alpha (\bar{x}_{le}/c_{ref})}^{C_{m,vle}} + \overbrace{K_{v,se} \sin^2\alpha (\bar{x}_{se}/c_{ref})}^{C_{m,vse}} \tag{4}$$

where the particular $\bar{x}$-terms equal $x_{ref} - x_{c,i}$. The next section deals with vortex lift at subsonic speeds.

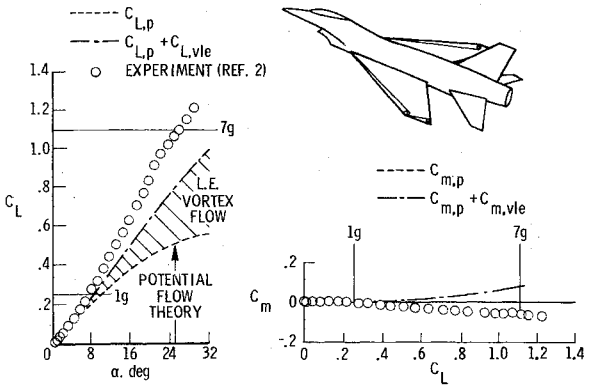

Fig. 1 Effect of vortex flows on wing aerodynamic characteristics.

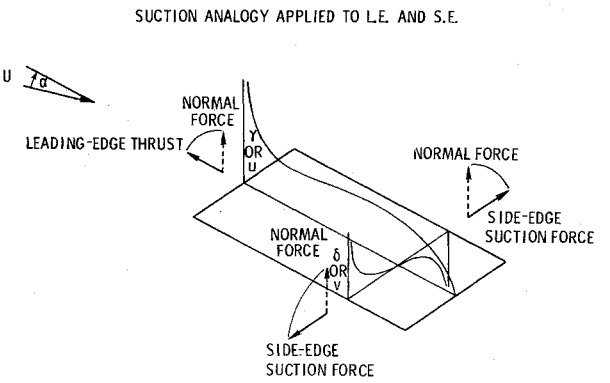

Fig. 2 Vortex-lift concept: suction analogy applied to L.E. and S.E.

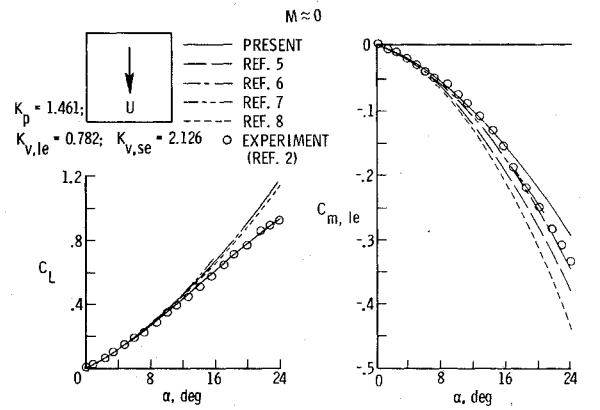

Fig. 3 Aerodynamic characteristics of $A = 1$ rectangular wing; $M \approx 0$.

Subsonic Vortex Lift

Comparisons

Figures 3, 4, and 5 present comparisons of experimental and theoretical subsonic aerodynamic characteristics of rectangular, sheared rectangular, and cropped-delta wings, respectively. Also shown are the magnitudes of the potential and vortex-lift factors as determined by the method of Ref. 2.

Figure 3 shows that the present method estimates the $A = 1$ rectangular wing C_L vs α data of Ref. 2 better than the other methods. (See Ref. 2 for a discussion of these other methods.[5-8]) The figure also shows that the $C_{m,le}$ vs α are better estimated by the present method up to $\alpha \approx 16°$. For higher angles of attack, the data show a larger nose-down moment than the present method estimates. This can be attributed in part to an assumption in the present method that the leading-edge vortex lift will always act at the leading edge and not move rearward with increasing angle of attack as the real vortex lift does.

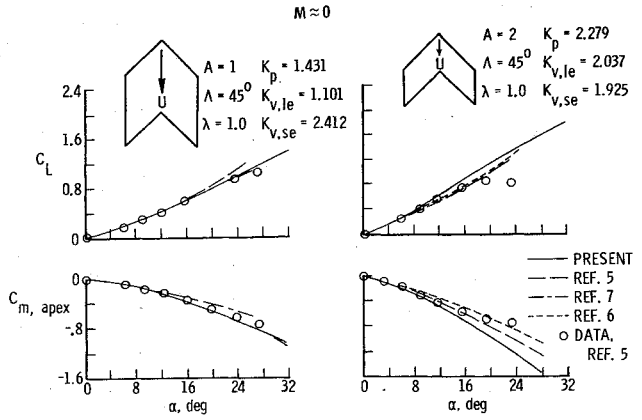

Fig. 4 Aerodynamic characteristics of two sheared rectangular wings; $M \approx 0$.

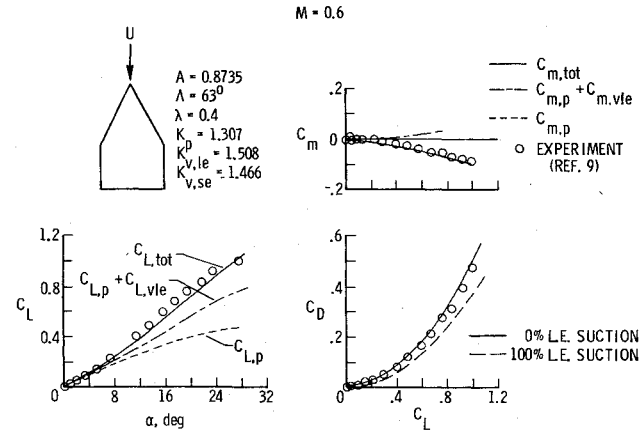

Fig. 5 Aerodynamic characteristics of a cropped-delta wing; $M = 0.6$.

Figure 4 shows that, for the $A = 1$ sheared wing, the present method estimates the C_L vs α and $C_{m,\text{apex}}$ vs α data of Ref. 5 as well or better than the methods of Gersten[5] and Belotserkovskii.[7] For the $A = 2$ sheared wing, no one method works well over the entire α-range, although up to $\alpha \approx 12°$, the C_L and $C_{m,\text{apex}}$ data are slightly better estimated by the present and Gersten's[5] methods. The falloff in measured lift and the more nose-up moment which occur for $\alpha > 12°$ indicate a lack of reattachment of the separated flow, or a breakdown in the shed-vortex system in the vicinity of the tip-trailing edge. Neither of these is accounted for in the present method, hence it would not be expected to estimate the data well in that α-range.

The C_L vs α graph for the cropped-delta wing at $M = 0.6$ show in Fig. 5 is an example of where the present method slightly underestimates the data.[9] This underestimation is attributed in Ref. 2 to additional induced effects associated with the actual shed-vortex system which have not been taken into account. These effects are attributed to the persistence of the leading-edge-vortex system in particular, the well-defined core region acting downstream from where the system was generated. It can, therefore, give rise to vortex lifts in excess of those estimated which are based on the vortex systems only acting along the edges where they are generated. Efforts are underway which will quantify these effects.

The C_m vs C_L and the C_D vs C_L graphs of Fig. 5 show an improvement in the data estimation when compared with the combination of potential flow and leading-edge-vortex flow, or potential flow alone. In particular, the inclusion of the side-edge-vortex lift in the C_m estimates provides a needed nose-down contribution previously lacking.†

†The C_D theoretical estimates given include the $C'_{D,o}$ term.

$K_{v,se}$ and $\Delta x/c_t$ Variations

The variations of $K_{v,se}$ and $\Delta x/c_t$ with $A\beta$ are given in Fig. 6 for cropped-delta wings at subsonic speeds by the method of Ref. 2 for a range of pertinent parameters. These are shown to illustrate the magnitudes and trends of $K_{v,se}$ and $\Delta x/c_t$ for an interesting class of wings. From the figure, it can be seen that, in general, $K_{v,se}$ increases with: 1) increasing taper ratio; 2) decreasing $A\beta$; or 3) increasing transformed-leading-edge sweep. As $A\beta \to 0$, $K_{v,se} \to \pi$. The chordwise centroid of side-edge-vortex lift, in general, moves forward with: 1) increasing transformed-leading-edge sweep; and 2) reduction in $A\beta$. As $A\beta \to 0$, $\Delta x/c_t \to 0.50$.

A separate analysis has shown that $K_{v,se}$ and $\Delta x/c_t$ for a wing at a subsonic Mach number have the same values as computed for the equivalent incompressible wing, obtained by using the Prandtl-Glauert compressibility factor. Furthermore, the sum of the vortex-lift factors at a subsonic Mach number can be written at a constant value of $A\beta$ as

$$K_{v,\text{tot}} = K_{v,se} + (K_{v,le}/f_M) \tag{5}$$

where

$$f_M = \sec \Lambda / (\beta^2 + \tan^2 \Lambda)^{1/2} \tag{6}$$

which is given in Ref. 10. The next section deals with vortex lift at supersonic speeds.

Supersonic Vortex Lift

Evidence

Polhamus[11] developed the following equation for delta wings at supersonic speeds

$$K_{v,le} = \frac{\pi[(16 - A^2B^2)(A^2 - 16)]^{1/2}}{16E^2} \tag{7}$$

and found reasonable agreement with experimental data on an $A = 1$ delta wing at $M = 1.97$ and 3.3.

On the left side of Fig. 7, a comparison of unpublished experimental data and the present method for an $A = 0.5$ delta wing at $M = 1.5$ is made. The comparison shows good agreement between the data and theory for $\alpha \leq 14°$ and, therefore, provides another example of leading-edge-vortex lift at supersonic speeds. The data are seen to be overestimated for $\alpha > 14°$, which indicates that the asymmetrical location of the model within its apex Mach cone due to increasing angle of attack is beginning to have a noticeable reducing effect on the upwash field around the leading edge, and, consequently, on $K_{v,le}$. The present method makes no provision for $K_{v,le}$ changing with α.

On the right side of Fig. 7 is shown the variation of c_n with α for an $A = 2$ rectangular wing at $M = 1.45$ obtained from Ref. 12 at two spanwise locations, one within and one outside the tip Mach cone. It can be seen that the c_n vs α variation outside the tip cone is well estimated by the potential flow theory of Ref. 13, whereas, within the tip cone the estimate of the data is too small. The insert of $\Delta C_{p,u}$ vs α at $2y/b = 0.875$ and $x/c = 0.953$ shows that within the tip cone a nonlinear variation in the upper surface pressure coefficient with α occurs of the type associated with vortex flows at subsonic speeds. The experimental c_n vs α curve at $2y/b = 0.875$ (short dashes) shows a similar nonlinear variation, although not as extreme as that noted for the $\Delta C_{p,u}$ graph shown. The reduction in the nonlinear behavior is attributed to: 1) the $\Delta C_{p,u}$ values measured ahead of the illustrated location demonstrating a smaller amount of nonlinear variation with α; and 2) the modifying effect of the lower surface pressure in the computation of c_n. The difference in c_n between the potential theory estimate and the data is, therefore, attributed to vortex lift which comes from the side edges located within the tip cones.

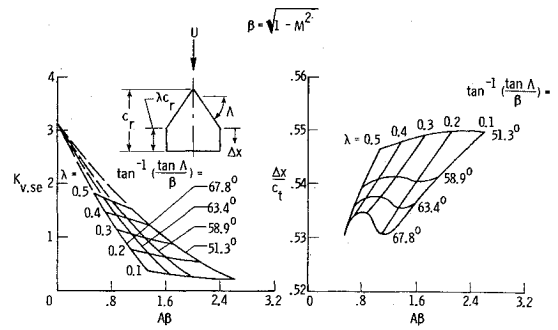

Fig. 6 Theoretical values of $K_{v,se}$ and $\Delta x/c_t$ for cropped-delta wings.

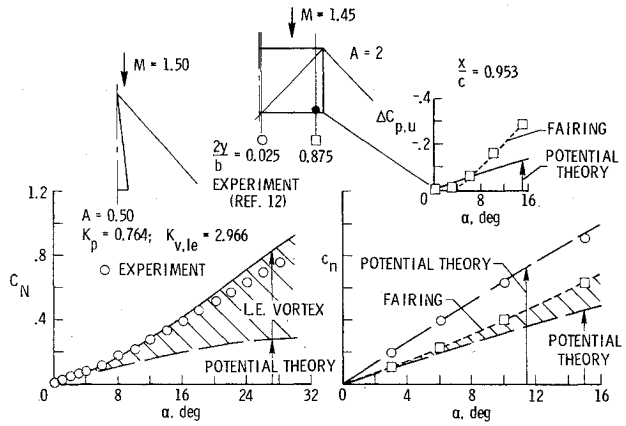

Fig. 7 Vortex lift at supersonic speeds.

Hence, the calculation of the attached flow side force and the utilization of a generalized-suction-analogy provide a means of estimating this lift effect. The next section discusses the computation of this vortex lift factor and its chordwise centroid.

$K_{v,se}$ and $\Delta x/c_t$ Variations

Figure 8 presents the variation of $K_{v,se}$ and $\Delta x/c_t$ for cropped arrow wings having subsonic leading edges and sonic trailing edges. The analytic expressions for these variables were developed by employing the velocity potential associated with angle of attack within the tip cone of cropped wings given in Ref. 14. The velocity potential is used to determine the induced side flow velocity from which $K_{v,se}$ is determined by a process similar to that given in Ref. 2. For the geometry specified previously, the expression for $K_{v,se}$ is

$$K_{v,se}=\frac{4c_t'(4+c_t')}{\pi[c_t'+(1-m)/2](1+m)} \tag{8}$$

where

$$m=B\cot\Lambda \tag{9}$$

$$c_t'=\frac{c_t}{b/2}\cot\Lambda \tag{10}$$

$$S_{\text{ref}}=(b^2/2)\tan\Lambda[c_t'+(1-m)/2] \tag{11}$$

with the restriction that the tip cones from the right and left wing panels not intersect ahead of the trailing edge.‡ By simply using an area ratio, both the graph and expression can be extended to estimate $K_{v,se}$ for cropped planforms having subsonic leading edges and supersonic trailing edges.

‡$m=1$ corresponds to a sonic leading edge.

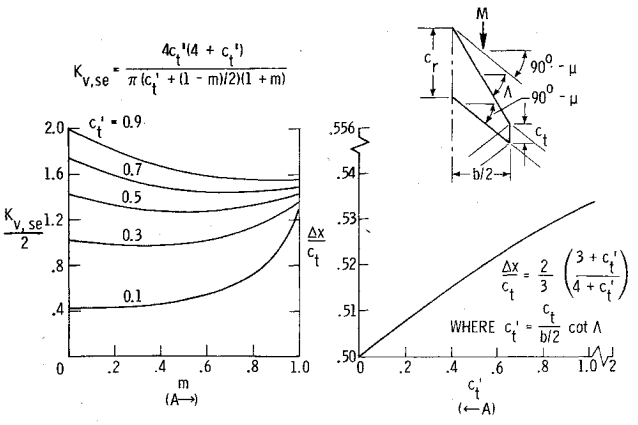

Fig. 8 Theoretical values of $K_{v,se}$ and $\Delta x/c_t$ for wings with subsonic leading edges and sonic trailing edges.

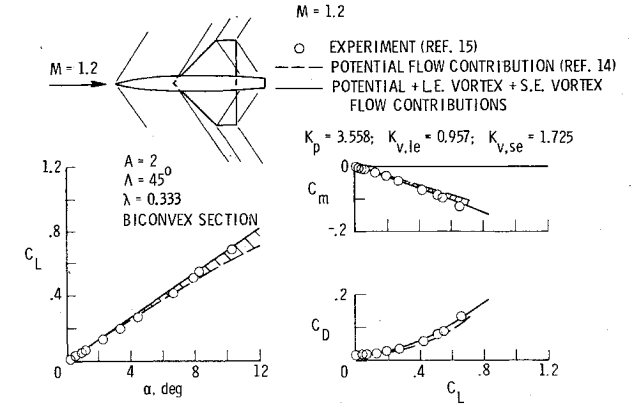

Fig. 9 Aerodynamic characteristics of a cropped-delta wing body; $M=1.2$.

The expression for $\Delta x/c_t$ is

$$\frac{\Delta x}{c_t}=\frac{2}{3}\left(\frac{3+c_t'}{4+c_t'}\right) \tag{12}$$

and can be seen to be independent of Mach number. This variable ranges from 0.50 for $c_t'=0$, (meaningless, since $K_{v,se}=0$), to 2/3 for $c_t'\to\infty$.

The effect of aspect ratio on these two variables can be deduced by examining the equation for S_{ref} (Eq. (11)). This equation shows that increases in aspect ratio occur for increasing m or decreasing c_t'.

For rectangular wings, the expressions for $K_{v,se}$ and $\Delta x/c_t$ can be written as

$$K_{v,se}=\delta/[\pi A(M^2-1)^{1/2}] \tag{13}$$

and

$$\Delta x/c_t=2/3 \tag{14}$$

It should be noted that at the lower supersonic Mach numbers: 1) larger amounts of vortex lift will be estimated at a fixed α, and 2) vacuum limit on the leeward surface and asymmetrical Mach cone reductions will be less noticeable over a larger α-range.

Comparison

Figure 9 presents a comparison of the aerodynamic characteristics obtained on a cropped delta-wing-body model tested at $M=1.2$ (Ref. 15) with those of the present method for the wing alone at the same Mach number. The comparison shows that the inclusion of the leading- and side-edge vortex-lift effects leads to improved agreement. Also, from the figure it can be seen that $K_{v,se}$ is almost twice that of $K_{v,le}$.

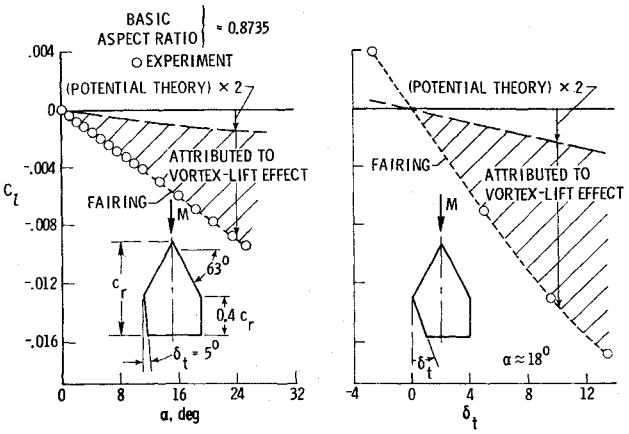

Fig. 10 Asymmetrical vortex lift used for roll control of cropped-delta wing at $M = 0.2$.

The pitching-moment contributions are obtained by having the vortex lifts act at their respective chordwise centroids, (2/3) $(b/2)$ tan Λ for the leading edge, and $(\Delta x/c_t)c_t$ for the side edge, and by performing the analytic surface integration of the potential flow lifting pressure (given in Ref. 14) with its chordwise position both within and outside the tip cone (see Ref. 16).

The potential theory drag curve contains $C_{D,o}$, and is obtained for full leading-edge suction with no separation around the side edges. The other theoretical drag curve also includes $C_{D,o}$.

Vortex Lift for Roll Control

Figure 5 illustrates the large amount of lift associated with the vortex flow around the side edges. Hence, it was hypothesized that, if there was a way of turning off or weakening the vortex flow on one wing panel, a significant amount of rolling moment could be produced, especially at the higher angles of attack where ailerons are generally ineffective. Thus, a proof-of-concept wind-tunnel program was recently undertaken to simulate a variable tip device which would be pivoted and retracted inside the wing. (This simulation was accomplished by testing asymmetrical models which were beveled symmetrically along all edges.) There should be two effects of the planform changes and they are: 1) the loss in area onto which the shed-vortex flow can act; and 2) a reduction in strength of the shed vortex due to a loss of vortex flow from the side edge. The latter is due to the side edge no longer being streamwise but instead oriented to act like a trailing edge.

The results of these tests are shown in Fig. 10 as C_l vs α at a constant δ_t, and as C_l vs δ_t at a constant α. The potential theory estimates of the asymmetrical model rolling-moment coefficients are obtained from the combinations of symmetrical model analyses using the method of Ref. 3, and are seen to be only a small fraction of the total. The difference between the potential theory and the data is attributed to the asymmetrical vortex lift effects. These data are particularly interesting in that they: 1) substantiate a procedure for achieving large rolling-moment coefficients at the higher angles of attack; and 2) would provide for high roll rates at various combinations of α and δ_t. In addition to providing roll control, this simulated control device produces generally favorable yawing moments (no shown). Estimating techniques are being developed to assist in the analysis of these data and the generalization of these effects to other planforms of the same type.

Conclusions

Wings having vortex flows around leading and side edges at subsonic and supersonic speeds have been studied by using the suction analogy. From the resulting comparisons of predicted and experimental data and other methods, as well as theoretical investigations undertaken, the following conclusions have been made: 1) The present method predicts subsonic wing static longitudinal aerodynamic data as well as, or better than, other methods. 2) The underestimation of lift for a cropped-delta wing is attributed to the persistence of the leading-edge-vortex system over the aft part of the wing, which is, of course, downstream from where the vortex system originates. 3) The side-edge-vortex-lift factor $K_{v,se}$ and its chordwise centroid are constant at subsonic speed for a fixed value of (aspect ratio) times $[1 - (\text{Mach number})^2]^{1/2}$ and planform type. 4) Side-edge-vortex-lift effects do appear at supersonic speeds and the overall effects can be estimated. 5) The variations of $K_{v,se}$ and its chordwise centroid at supersonic speeds can be written in closed form for classes of wings. 6) Tip raking on a cropped-delta wing has been shown to be an effective way to achieve roll control at high angles of attack and subsonic speeds.

References

[1] Polhamus, E. C., "A Concept of the Vortex Lift of Sharp-Edge Delta Wings Based on a Leading-Edge-Suction Analogy," NASA TN D-3767, 1966.

[2] Lamar, J. E., "Extension of Leading-Edge-Suction Analogy to Wings With Separated Flow Around the Side Edges at Subsonic Speeds," NASA TR R-428, 1974.

[3] Lamar, J. E., "A Modified Multhopp Approach for Predicting Lifting Pressures and Camber Shape for Composite Planforms in Subsonic Flow," NASA TN D-4427, 1968.

[4] Bradley, R. G., Smith, C. W., and Bhateley, I. C., "Vortex-Lift Prediction for Complex Wing Planforms," *Journal of Aircraft*, Vol. 10, June 1973, pp. 379-381.

[5] Gersten, K., "Calculation of Non-Linear Aerodynamic Stability Derivative of Aeroplanes," AGARD Rep. 342, April 1961.

[6] Garner, H. C. and Lehrian, D. E., "Non-Linear Theory of Steady Forces on Wings With Leading-Edge Flow Separation," NPL Aero Rep. 1059, Aeronautical Research Council, London, Feb. 1963.

[7] Belotserkovskii, S. M. (J. W. Palmer, trans.), "Calculation of the Flow About Wings of Arbitrary Planform at a Wide Range of Angles of Attack," Library Translation No. 1433, Royal Aircraft Establishment, Farnsborough, Feb. 1970.

[8] Flax, A. H. and Lawrence, H. R., "The Aerodynamics of Low-Aspect-Ratio Wings and Wing-Body Combination," *Third Anglo-American Aeronautical Conference*, J. Bradbrooke and E. C. Pike, eds., Royal Aeronautical Society, 1952, pp. 363-398.

[9] Emerson, H. F., "Wind-Tunnel Investigation of the Effect of Clipping the Tips of Triangular Wings of Different Thickness, Camber, and Aspect Ratio-Transonic Bump Method," NACA TN 3671, 1956.

[10] Polhamus, E. C., "Charts for Predicting the Subsonic Vortex-Lift Characteristics of Arrow, Delta, and Diamond Wings," NASA TN D-6243, 1971.

[11] Polhamus, E. C., "Predictions of Vortex Lift Characteristics by a Leading-Edge Suction Analogy," *Journal of Aircraft*, Vol. 8, April 1971, pp. 193-199.

[12] Kaattari, G. E., "Pressure Distributions on Triangular and Rectangular Wings to High Angles of Attack – Mach Numbers 1.45 and 1.97," NACA RM A54D19, 1954.

[13] Woodward, F. A., "Analysis and Design of Wing-Body Combinations at Subsonic and Supersonic Speeds," *Journal of Aircraft*, Vol. 5, Nov. 1968, pp. 528-534.

[14] Malvestuto, F. S., Jr., Margolis, K., and Ribner, H. S., "Theoretical Lift and Damping in Roll at Supersonic Speeds of Thin Sweptback Tapered Wings and Streamwise Tips, Subsonic Leading Edges, and Supersonic Trailing Edges," NACA Rept. 970, 1950.

[15] Hightower, R. C., "Lift, Drag, and Pitching Moment of Low-Aspect-Ratio Wings at Subsonic and Supersonic Speeds – Comparison of Three Wings of Aspect Ratio 2 of Rectangular, Swept-Back, and Triangular Planform, Including Effects of Thickness Distribution," NACA RM A52L02, 1953.

[16] Malvestuto, F. S., Jr. and Hoover, D. M., "Lift and Pitching Derivatives of Thin Sweptback Tapered Wings with Streamwise Tips and Subsonic Leading Edges at Supersonic Speeds," NACA TN 2294, 1951.